A *Shigella* type 3 effector protein co-opts host inositol pyrophosphates for activity

Thomas E. Wood,[1,2,†] Jessica M. Yoon,[3,5,†] Heather D. Eshleman,[1,2,6] Daniel J. Slade,[4] Cammie F. Lesser,[1,2] Marcia B. Goldberg[1,2,*]

[1]Department of Medicine, Division of Infectious Diseases, Massachusetts General Hospital, Boston, Massachusetts, USA.

[2]Department of Microbiology, Blavatnik Institute, Harvard Medical School, Boston, Massachusetts, USA.

[3]Department of Molecular and Cellular Biology, Harvard University, Cambridge, Massachusetts, USA.

[4]Department of Biochemistry, Virginia Polytechnic Institute and State University, Blacksburg, Virginia, USA

[5]Present address: Office of Response and Recovery, Federal Emergency Management Agency, Washington, D.C., USA

[6]Present address: Lexical Intelligence, LLC, Rockville, Maryland, USA

[†]These authors contributed equally to this work.

[*]For correspondence: E-mail: marcia.goldberg@mgh.harvard.edu Tel: +1 617-525-4820.

Abstract

Shigella spp. cause diarrhea by invading human intestinal epithelial cells. Effector proteins delivered into target host cells by the *Shigella* type 3 secretion system modulate host signaling pathways and processes in a manner that promotes infection. The effector OspB activates mTOR, the central cellular regulator of growth and metabolism, and potentiates the inhibition of mTOR by rapamycin. The net effect of OspB on cell monolayers is cell proliferation at infectious foci. To gain insights into the mechanism by which OspB potentiates rapamycin inhibition of mTOR, we employ *in silico* analyses to identify putative catalytic residues of OspB and show that a conserved cysteine-histidine dyad is required for this activity of OspB. In a screen of an over-expression library in *Saccharomyces cerevisiae*, we identify a dependency of OspB activity on inositol pyrophosphates, a class of eukaryotic secondary messengers that are distinct from the inositol phosphates known to act as cofactors for bacterial cysteine proteases. We show that inositol pyrophosphates are required for OspB activity not only in yeast, but also in mammalian cells - the first demonstration of inositol pyrophosphates being required for virulence of a bacterial pathogen *in vivo*.

Introduction

Shigella spp. are the etiological agents of bacillary dysentery, accounting for one of the leading causes of mortality from diarrheal disease (Khalil et al., 2018). These Gram-negative bacterial pathogens invade the intestinal epithelium, establishing a replicative niche within colonic epithelial cells and triggering an acute inflammatory immune response (Carayol & Tran Van Nhieu, 2013). The type 3 secretion system (T3SS) is required for *S. flexneri* infection, facilitating invasion and bacterial multiplication through the delivery into host cells of effector proteins that subvert cellular signaling pathways. Effector proteins also promote the cell-to-cell spread of intracellular *Shigella*, whereby it disseminates throughout the intestinal epithelium (Agaisse, 2016).

The T3SS effector protein OspB restricts the intercellular spread of *S. flexneri* by activating mammalian target of rapamycin (mTOR), the master regulator of cellular growth (Lu et al., 2015). OspB-mediated activation of mTOR promotes survival and proliferation of infected host epithelial cells, which may supply further niches for the replicating bacteria. Other phenotypes have also been described for OspB, such as dampening the innate immune response *via* MAP kinase and NF-κB signaling and modulating cytokine release (Ambrosi et al., 2015; Fukazawa et al., 2008; Zurawski, Mumy, Faherty, McCormick, & Maurelli, 2009).

To gain insights into the mechanisms of OspB activity, we explored similarities among OspB and its homologs and conducted a genome-wide screen for host factors necessary for its activity. We identified the catalytic residues of OspB through bioinformatic analysis and assessed their requirement for OspB activity. Exploiting a *Saccharomyces cerevisiae* expression system, we determined that inositol phosphate biosynthesis is a process critical to OspB activity. Genetic analysis of this pathway demonstrated that inositol pyrophosphates, rather than inositol phosphates, are necessary for OspB function, suggesting a role for inositol pyrophosphates during bacterial infection.

Results and Discussion

OspB exhibits structural homology to cysteine proteases

To improve our understanding of the mechanism of action of OspB, we performed *in silico* analyses of its amino acid sequence. This analysis revealed that OspB shares 27-30% sequence identity with the cysteine protease domains (CPD) of the large clostridial cytotoxins TcdA and TcdB of *Clostridioides difficile* and the multifunctional autoprocessing repeats-in-toxin (MARTX) RtxA toxins of *Vibrio cholerae* and *V. vulnificus* (**Figure 1a**). TcdA, TcdB and RtxA are modular toxins that upon endocytosis into the host cell undergo autoproteolysis, which releases toxin domains that subvert cellular processes by inducing actin depolymerization and altering GTPase signaling (Fullner & Mekalanos, 2000; Just et al., 1995). In contrast to these large cytotoxins, OspB is small (288 amino acids; 32 kD) and in cells, we found no evidence for OspB autoprocessing (**Figure S1**).

The cysteine and histidine residues required for the proteolytic activity of the CPDs are conserved in OspB and the orthologous T3SS effector protein of *V. parahaemolyticus* VPA1380 (Calder et al., 2014; Egerer, Giesemann, Jank, Satchell, & Aktories, 2007; Sheahan, Cordero, & Satchell, 2007) (**Figure 1a**). Indeed, the tertiary structure of OspB can be modelled on the CPDs of RtxA and TcdA with 96% and 62% confidence, respectively, with conservation of the positions of their catalytic residues with C184 and H144 of OspB (**Figure 1b**). Mutagenesis studies of TcdA showed that in addition to C700 and H655, D589 is required for autoprocessing through proton abstraction from the histidine in the active site, whereas the analogous aspartic acid residue in RtxA is not required for its activity (Prochazkova et al., 2009; Pruitt et al., 2009). Rather, the catalytic residues of RtxA comprise solely of the C3568-H3519 dyad. In OspB an aspartic acid residue (D108) is present at the equivalent position of $D589^{TcdA}$ and was therefore a candidate for involvement in catalysis (**Figure 1b**).

The alignment of OspB with RtxA and TcdA suggested that OspB residues C184 and H144, and potentially D108, may be required for OspB activity. A quantitative assay in yeast strains expressing *S. flexneri* effector proteins previously demonstrated that OspB causes growth inhibition of yeast in the presence of the cellular stressor caffeine (Slagowski, Kramer, Morrison, LaBaer, & Lesser, 2008). We

utilized this assay to probe the role of the putative catalytic residues in OspB activity. Whereas expression of wild type OspB elicits a drastic growth defect in the presence of caffeine, mutation of either C184 or H144 completely abrogated toxicity (**Figure 1c**). On the other hand, alanine substitution of D108 did not rescue yeast growth. These results indicate that the function of OspB requires both a cysteine and a histidine residue and is independent of D108, similar to the cysteine-histidine catalytic dyad of the CPD of RtxA.

Among the effects of caffeine on cellular processes, in yeast, inhibition of TOR is described as an important mode of action for this compound (Reinke, Chen, Aronova, & Powers, 2006). To determine whether TOR plays a role in OspB-dependent growth inhibition of yeast, we replaced caffeine in the media with rapamycin, which unlike caffeine is a specific inhibitor of TOR. As with caffeine, the presence of rapamycin sensitized yeast to growth inhibition by OspB in a manner that depended on residues C184 and H144 (**Figure 1c**).

These results indicate that the activity of OspB in yeast results in hypersensitivity to TOR inhibition, either by caffeine or by rapamycin, which mirrors our previous findings that OspB potentiates rapamycin inhibition of growth in mammalian cells (Lu et al., 2015). Functional analysis of point mutations in OspB derivatives shows that this modulation of the TOR pathway depends on the predicted catalytic dyad of C184 and H144, bolstering our predictions for the tertiary structure of OspB as a structural homolog of the cysteine protease domains of several modular bacterial toxins. Furthermore, the presence of similar OspB-dependent phenotypes in both yeast and mammalian cells with respect to sensitization to TOR inhibition demonstrates that yeast present a reasonable model for investigating the mechanism of OspB activity.

In yeast, inositol pyrophosphate biosynthesis is necessary for OspB-mediated growth inhibition

With the goal of identifying factors required for OspB activity, we screened a *S. cerevisiae* over-expression library (Sopko et al., 2006) for genes that rescued OspB inhibition of yeast growth in the presence of caffeine (**Figure 2a**). The OspB-mediated growth defect was suppressed by over-expression of several genes, including two in the inositol phosphate biosynthetic pathway, *DDP1*

and *SIW14* (**Table S1**). Of note, the CPDs of RtxA and TcdA bind inositol hexakisphosphate (IP_6) (**Figure 1b**) and require it for cysteine protease activity *in vitro* (Prochazkova & Satchell, 2008; Reineke et al., 2007). Therefore, we investigated whether OspB also recruits an inositol phosphate species as a cofactor. Introduction of a plasmid over-expressing either *DDP1* or *SIW14* into a yeast strain that constitutively produces OspB resulted in complete rescue of the OspB-mediated growth defect, whereas the empty over-expression vector control had no effect (**Figure 2b**). *DDP1* and *SIW14* each encode a phosphatase that hydrolyzes β-phosphates of inositol pyrophosphate species (Kilari, Weaver, Shears, & Safrany, 2013; Safrany et al., 1999; Steidle et al., 2016) (**Figure 2c**). Inositol pyrophosphate molecules may contain up to eight phosphate groups with at least one phosphoanhydride-bonded pyrophosphate moiety, as opposed to the six individually ester-bonded phosphate groups present on IP_6 (**Figure 2c**). These results thus indicate that in yeast cells, the presence of inositol pyrophosphates, rather than IP_6 itself, may be required for OspB function.

Ddp1p and Siw14p have preferences for the β-phosphate at the 1- and 5-positions, respectively, and can dephosphorylate 1,5-IP_8, 1-IP_7 and 5-IP_7 to produce IP_6 (Kilari et al., 2013; Steidle et al., 2016; Wang, Gu, Rolfes, Jessen, & Shears, 2018) (**Figure 2c**). A further inositol pyrophosphate species, PP-IP_4, can be produced from 5-kinase activity on the substrate IP_5 (Saiardi, Caffrey, Snyder, & Shears, 2000). To discriminate whether PP-IP_4 or an IP_6-derived inositol pyrophosphate species is involved in OspB-mediated growth inhibition, we tested the effect on the OspB phenotype of a deletion in *IPK1*, which encodes the 2-kinase that generates IP_6 from IP_5 (York, Odom, Murphy, Ives, & Wente, 1999). Deletion of *IPK1* suppressed OspB-mediated sensitization to caffeine (**Figure 2d**), demonstrating that the cofactor(s) required for OspB function in yeast cells is specifically one or more inositol pyrophosphate species synthesized from the precursor IP_6.

In mammalian cells, OspB activity depends on inositol pyrophosphates

The inositol phosphate biosynthetic pathway is conserved throughout eukaryotes. However, in mammalian cells, several isoforms exist of the enzymes that carry out each step of the biosynthetic pathway. IP_6 and 1-IP_7 are phosphorylated at the 5-position by Kcs1p in yeast, whereas in mammalian cells this activity is conducted by isoforms 1, 2 and 3 of inositol hexakisphosphate kinase (IP6K1/2/3)

(Saiardi, Erdjument-Bromage, Snowman, Tempst, & Snyder, 1999; Shears, 2018) (**Figures 2d** and **3a**). Phosphorylation of the 1-position phosphate group of IP_6 and 5-IP_7 is catalyzed by the yeast enzyme Vip1p, of which the mammalian homologs are isoforms 1 and 2 of diphosphoinositol-pentakisphosphate kinase (PPIP5K1/2) (Choi, Williams, Cho, Falck, & Shears, 2007; Fridy, Otto, Dollins, & York, 2007; Mulugu et al., 2007). Biochemical analyses of inositol phosphate levels in mammalian cells reveal that aside from the major species IP_6, 5-IP_7 and 1,5-IP_8 are relatively abundant, whereas 1-IP_7 constitutes just 2% of cellular IP_7 (Gu, Wilson, Jessen, Saiardi, & Shears, 2016). Thus, the primary pathway of inositol pyrophosphate synthesis from IP_6 is thought to proceed *via* 5-IP_7 and to be catalyzed by IP6K enzymes.

To determine whether inositol pyrophosphates are required for OspB activity in mammalian cells, we examined OspB during infection with *S. flexneri*. When *Shigella* infects cell monolayers, it spreads from cell to cell using actin-based motility, with eventual death of the infected cells (Bernardini, Mounier, D'Hauteville, Coquis-Rondon, & Sansonetti, 1989; Carneiro et al., 2009). Over the course of 48-72 h of infection, bacterial spread creates central areas of cellular debris, known as plaques. By simultaneously activating mTOR-induced cell proliferation of viable cells at the periphery of the plaques, OspB restricts the total area of plaques formed by *S. flexneri* in cell monolayers (Lu et al., 2015). Consequently, an Δ*ospB* mutant produces larger plaques than the wild type strain. To test the role of inositol pyrophosphates in OspB activity in mammalian cells, we assessed the impact of the presence or absence of OspB on the area of spread of *S. flexneri* strains with severely reduced inositol pyrophosphate levels.

Most cellular 5-IP_7 is synthesized by isoform 1 of IP6K (IP6K1), such that in cells with a deletion in *IP6K1*, levels of inositol pyrophosphates are markedly reduced (Bhandari, Juluri, Resnick, & Snyder, 2008). A previously described (Lu et al., 2015), in $IP6K^{+/+}$ cells, wild type *S. flexneri* produced plaques that were significantly smaller than those of the Δ*ospB* mutant (**Figures 3b and c**). In contrast, in the absence of *IP6K1*, wild type *S. flexneri* produced plaques that were significantly larger than those it produced in $IP6K1^{+/+}$ cells. Moreover, in $IP6K1^{-/-}$ cells, the plaques produced by the wild type strain were similar in size to those produced by the Δ*ospB* mutant. These findings demonstrate that inositol

pyrophosphates are necessary for the ability of OspB to restrict plaque size, indicating that, as in yeast cells, OspB depends on one or more of these eukaryotic signaling molecules for full activity in mammalian cells.

Whereas IP_7 and IP_8 species have been shown to be important secondary messengers, influencing the cell cycle, cellular energy levels and vesicle trafficking (Chanduri et al., 2016; Lee, Mulugu, York, & O'Shea, 2007; Szijgyarto, Garedew, Azevedo, & Saiardi, 2011), to the best of our knowledge, this is the first demonstration of these molecules being required for bacterial virulence. A described virulence-associated role for inositol pyrophosphates is in innate immune responses to viral pathogens, whereby production of 1-IP_7 by *PPIP5K2* promotes the type I interferon response (Pulloor et al., 2014). By contrast, here we show that the *S. flexneri* T3SS effector protein co-opts inositol pyrophosphates to facilitate infection, utilizing the host signaling molecule to the advantage of the bacterium.

Given the sequence similarity and predicted structural homology of OspB to the CPDs of TcdA, TcbB and RtxA (**Figure 1**), and the structural and biochemical evidence that IP_6 serves as a cofactor for the cysteine protease domains of these toxins, the mechanism by which inositol pyrophosphates are required for OspB activity is presumably analogous to the role of IP_6 in TcdA, TcbB and RtxA, namely as a cofactor. The negatively-charged inositol phosphate cofactor binds to a pocket in these CPDs that consists of several positively-charged residues (predominantly lysines and arginines) and cofactor binding induces a conformational change in the active site, which in turn activates proteolysis (Lupardus, Shen, Bogyo, & Garcia, 2008; Prochazkova et al., 2009; Prochazkova & Satchell, 2008; Pruitt et al., 2009; Shen et al., 2011). OspB is also rich in positively-charged residues; the 288-residue protein contains 31 lysines and 8 arginines. However, the sequence of OspB that aligns with RtxA and TcdA does not encompass the RtxA or TcdA IP_6-binding pocket, making it challenging to predict the inositol pyrophosphate binding pocket in OspB.

Several bacterial virulence factors, such as the T3SS effectors YopJ of *Yersinia* spp., IcsB of *S. flexneri*, and the aforementioned MARTX and clostridial toxins, are activated by IP_6 *in vitro* (Liu et al., 2018; Mittal, Peak-Chew, Sade, Vallis, & McMahon, 2010; Prochazkova & Satchell, 2008; Reineke et al., 2007). However, which inositol phosphate species activates these bacterial proteins *in situ* in the host

cell cytosol has not been explicitly determined. One report into the activation of TcdB found that *in vitro*, IP_7 induces autoproteolysis more efficiently than IP_6 (Savidge et al., 2011), raising the possibility that *in vivo*, an inositol pyrophosphate may be the preferred cofactor.

We show that the suppression of OspB-mediated yeast growth inhibition in the absence of *ipk1* indicates that IP_6, IP_7 and/or IP_8 are needed for OspB activity in yeast. Furthermore, through over-expression of *DDP1* or *SIW14*, which reduces cellular levels of inositol pyrophosphates, we demonstrated that IP_6 is unlikely to be the relevant inositol phosphate species activating OspB (**Figure 2**). VPA1380, the *V. parahaemolyticus* ortholog of OspB, requires *IPK1* for its activity, and mutagenesis of predicted IP_6-binding residues abrogated its function (Calder et al., 2014). Since in addition to being unable to produce IP_6, an *ipk1*Δ mutant is unable to produce IP_7 or IP_8, it is plausible that inositol pyrophosphates are the preferred cofactors for activating all members of the OspB family of effector proteins.

With current data, we cannot discriminate which single species or whether multiple species among 1-IP_7, 5-IP_7 and/or 1,5-IP_8 is/are functioning as a cofactor of OspB. We also cannot eliminate the possibilities that the biosynthetic enzymes themselves are playing a role or that modulation of inositol pyrophosphates levels has an indirect effect on OspB activity; however, we believe that the preponderance of evidence weighs in favor of a physical association between OspB and inositol pyrophosphates. It is apparent that cofactor promiscuity exists *in vitro* and that the relative concentrations of inositol phosphates species and sub-cellular localization and sequestration in cells will be important determinants in cofactor preference. In conclusion, we present the first demonstration of the exploitation of the host inositol pyrophosphates by a bacterial virulence factor *in vivo*, furthering our understanding of the utilization of host cofactors by pathogens during infection.

Experimental Procedures

Growth conditions and cell culture

S. flexneri serotype 2a wild type strain 2457T and its isogenic *ospB* mutant have been described (Labrec, Schneider, Magnani, & Formal, 1964; Lu et al., 2015). Bacteria were isolated from single red colonies on agar containing Congo red and were grown in tryptic soy broth at 37 °C with agitation. *E. coli* DH10B (Grant, Jessee, Bloom, & Hanahan, 1990) was used as the routine cloning host and was grown in Luria broth at 37 °C. *S. cerevisiae* S288C was used as the heterologous expression host to probe the roles of host proteins in the function of OspB and was routinely cultured at 30 °C in yeast extract-peptone-dextrose (YPD) broth or in synthetic selective media (MP Biomedicals) lacking histidine, uracil and/or leucine for auxotrophic selection. 1.5 % (w/v) agar was added for solid media formulations, and where appropriate, media was supplemented with 50 µg/ml ampicillin, 2% (w/v) D-glucose, 2% (w/v) D-galactose, 6 mM caffeine or 5 nM rapamycin.

IP6K1$^{+/+}$ and *IP6K1*$^{-/-}$ mouse embryonic fibroblast cell lines (provided by Dr Anutosh Chakraborty, St Louis University, St Louis, MO) were maintained in Dulbecco's modified Eagle medium (DMEM) (Gibco) supplemented with 10% (v/v) fetal bovine serum (FBS) at 37 °C with 5% CO_2. Inhibition of mTOR was achieved through the addition of 10 nM rapamycin to mammalian cell culture media.

Bioinformatic analyses

In silico modelling of the tertiary structure of OspB was conducted on the Phyre2 server (Kelley, Mezulis, Yates, Wass, & Sternberg, 2015), whereas alignment with the crystal structures of RtxA^{VC} (Lupardus et al., 2008) and TcdA (Pruitt et al., 2009) was achieved using the CEAlign algorithm within PyMol (Schrödinger, LLC). Protein sequences were retrieved from the non-redundant NCBI database and aligned using MUSCLE (Edgar, 2004) before manual curation to select the regions of interest.

Genetic manipulations

For expression of *ospB* in *S. cerevisiae*, the *ospB* gene from *S. flexneri* 2457T was cloned into the Gateway destination vector pAG413GPD-*EGFP-ccdB* (provided by Dr Susan Lindquist) to replace

the *EGFP* gene. Generation of OspB point mutants was achieved by splicing by overlap extension PCR using the following combinations of primers:
CCGTTTTACTTCAAGCGGCTCCGCTGATAAAGTGG and
CCACTTTATCAGCGGAGCCGCTTGAAGTAAAACGG for C184S;
5'-GGTTTATATTCTTGGGGCCGGTAGTCCTGGTTCTCATC and
5'-GATGAGAACCAGGACTACCGGCCCCAAGAATATAAACC for H144A;
5'- TAGTAATAAATAATGCTGATGACGCAT and
5'- ATGCGTCATCAGCATTATTTATTACTA for D108A. Allelic exchange was used to construct the *ipk1*Δ mutant in *S. cerevisiae* BY4741, replacing the gene with a *LEU2* cassette. The *LEU2* gene was amplified by PCR from the pRS315 vector using primers
5'-ACCAGTCGAAAATTGTCAGAGATAAGTTCCTTTTTTGAAAAGAAAGATCGTAACTGTG GGAATACTCAGG and
5'-TAATGTATGTGCATCTGCCAGTACCAAAGGTGGAAAGAAAAGTATACAGTTTTAAGCA AGGATTTTC. The resulting product was transformed into BY4741, and to select for homologous recombination, the yeast were grown on selective media. Successful integration into the *ipk1* locus was assessed by colony PCR using primers 5'-CACGTAGGAAAGCGA and
5'-CCCTTCGTTGAATATCG and by demonstration of loss of leucine auxotrophy. Yeast were transformed using the lithium acetate method.

Yeast growth assays and screen for suppressors of growth inhibition

Individual yeast transformants that constitutively express *ospB* or derivatives containing point mutations were grown in synthetic selective liquid media containing 2% D-glucose. To investigate the impact of OspB constructs on growth, yeast cells were washed and serially diluted four-fold in phosphate-buffered saline before 5 µl of each dilution were spotted on synthetic selective solid media. Media contained 2% D-glucose either without further additives or supplemented with 6 mM caffeine or 5 nM rapamycin. The role of the yeast *IPK1* gene was assessed similarly.

To screen for suppressors of OspB-mediated toxicity in *S. cerevisiae* by yeast gene over-expression, the strain BY4742 pAG413GPD-*ospB* was mated with the haploid GST-fusion yeast over-expression

library (YSC4423, Dharmacon) on YPD. The resulting diploids were selected by plating on non-inducing synthetic selective media containing 2% D-glucose. The screen was conducted by spotting in quadruplicate on inducing synthetic selective solid media containing 2% D-galactose and 6 mM caffeine. All steps in the screen were conducted in an automated manner as described previously (Slagowski et al., 2008). Suppressors were classified as strains which displayed qualitatively moderate to robust growth of all four spots on the caffeine plate four days after pinning. Direct analysis of suppressor genes *DDP1* and *SIW14* was achieved through plasmid isolation and transformation into BY4741 pAG413GPD-*ospB* and assayed as above by serial dilution onto media containing D-galactose.

Transfection

Transfection plasmids were constructed by cloning the *ospB* gene into the pCMV-*myc* vector at EcoRI and XhoI sites. A construct encoding OspB or its C184S derivative was also amplified with a C-terminal triple FLAG and hexahistidine tag and cloned into pcDNA3 at BamHI and XhoI sites. Cells were transfected with plasmids using FuGENE 6 (Promega) according to the manufacturer's instructions, and experimental samples were analyzed 24 h after transfection.

SDS-PAGE and immunoblotting

For immunoblot analysis, protein samples were separated by SDS-PAGE, transferred to nitrocellulose membranes and detected by western blot analysis using standard procedures. The antibodies used were peroxidase-conjugated anti-β-actin (A3854, Sigma; diluted to 1:10 000), anti-α-tubulin (sc-53030, Santa Cruz; diluted to 1:1000), anti-FLAG (F3165, Sigma; diluted to 1:1000), anti-myc (631206, Clontech; diluted to 1:1000) and anti-OspB (diluted to 1:10 000). The rabbit anti-OspB antibody was generated (Covance Inc.) against a 14-mer peptide of OspB located 18 residues from the C-terminus.

Plaque assays

Mouse embryonic fibroblasts were seeded in 6-well plates and infected with exponential phase *S. flexneri* strains at a multiplicity of infection of 0.004. Bacteria were centrifuged onto the cells at 830 *g* for 10 min before incubation for 50 min at 37 °C in 5% CO_2. The media was replaced with a 0.5% (w/v) agarose overlay in DMEM containing FBS and 25 µg/ml gentamicin to kill extracellular bacteria. After

287 setting at room temperature for 10 min, the infection was allowed to continue at 37 °C for 48 h, before
288 adding a 0.7% (w/v) agarose overlay in DMEM containing FBS, gentamicin and 0.002% (w/v) neutral
289 red dye. Infected monolayers were imaged using a scanner after a further 150 min incubation. Semi-
290 automated measurement of plaque area was conducted using FIJI (Schindelin et al., 2012) using a script
291 developed in-house. Statistically significant differences in plaque size was determined with the tests
292 described in the figure legend using Prism 8.0 (GraphPad).

Acknowledgements

We thank Austin C. Hachey and Yang Fu for technical assistance. We are grateful to Dr. Anutosh Chakraborty (St Louis University, St Louis, MO) and Prof. Solomon H. Snyder (Johns Hopkins Medical School, Baltimore, MD) for the gift of *IP6K1*$^{-/-}$ mouse embryonic fibroblasts. We thank Stephen B. Shears, Henning Jessen, and D. Borden Lacy for helpful discussions. This research was supported by Department of Defense grant TS160046 (to M.B.G.), funding from the Massachusetts General Hospital Executive Committee on Research (to M.B.G.), NIH grants T32 AI007061 and F32 AI131582 (to H.D.E.) and R01 AI064285 (to C.F.L.). The authors have no conflicts of interest.

References

Agaisse, H. (2016). Molecular and Cellular Mechanisms of *Shigella flexneri* Dissemination. *Frontiers in Cellular and Infection Microbiology*, *6*(March), 29. http://doi.org/10.3389/fcimb.2016.00029

Ambrosi, C., Pompili, M., Scribano, D., Limongi, D., Petrucca, A., Cannavacciuolo, S., … Nicoletti, M. (2015). The *Shigella flexneri* OspB effector: an early immunomodulator. *International Journal of Medical Microbiology*, *305*(1), 75–84. http://doi.org/10.1016/j.ijmm.2014.11.004

Bernardini, M. L., Mounier, J., D'Hauteville, H., Coquis-Rondon, M., & Sansonetti, P. J. (1989). Identification of *icsA*, a plasmid locus of *Shigella flexneri* that governs bacterial intra- and intercellular spread through interaction with F-actin. *Proceedings of the National Academy of Sciences of the United States of America*, *86*(10), 3867–71. http://doi.org/10.1073/pnas.86.10.3867

Bhandari, R., Juluri, K. R., Resnick, A. C., & Snyder, S. H. (2008). Gene deletion of inositol hexakisphosphate kinase 1 reveals inositol pyrophosphate regulation of insulin secretion, growth, and spermiogenesis. *Proceedings of the National Academy of Sciences of the United States of America*, *105*(7), 2349–53. http://doi.org/10.1073/pnas.0712227105

Calder, T., Kinch, L. N., Fernandez, J., Salomon, D., Grishin, N. V., & Orth, K. (2014). *Vibrio type* III effector VPA1380 is related to the cysteine protease domain of large bacterial toxins. *PLoS ONE*, *9*(8), e104387. http://doi.org/10.1371/journal.pone.0104387

Carayol, N., & Tran Van Nhieu, G. (2013). The inside story of *Shigella* invasion of intestinal epithelial cells. *Cold Spring Harbor Perspectives in Medicine*, *3*(10), a016717. http://doi.org/10.1101/cshperspect.a016717

Carneiro, L. A. M., Travassos, L. H., Soares, F., Tattoli, I., Magalhaes, J. G., Bozza, M. T., … Girardin, S. E. (2009). *Shigella* induces mitochondrial dysfunction and cell death in nonmyleoid cells. *Cell Host and Microbe*, *5*(2), 123–36. http://doi.org/10.1016/j.chom.2008.12.011

Chanduri, M., Rai, A., Malla, A. B., Wu, M., Fiedler, D., Mallik, R., & Bhandari, R. (2016). Inositol

hexakisphosphate kinase 1 (IP6K1) activity is required for cytoplasmic dynein-driven transport. *The Biochemical Journal*, *473*(19), 3031–47. http://doi.org/10.1042/BCJ20160610

Cherry, J. M., Hong, E. L., Amundsen, C., Balakrishnan, R., Binkley, G., Chan, E. T., … Wong, E. D. (2012). *Saccharomyces* Genome Database: the genomics resource of budding yeast. *Nucleic Acids Research*, *40*(Database issue), D700-5. http://doi.org/10.1093/nar/gkr1029

Choi, J. H., Williams, J., Cho, J., Falck, J. R., & Shears, S. B. (2007). Purification, sequencing, and molecular identification of a mammalian PP-InsP_5 kinase that is activated when cells are exposed to hyperosmotic stress. *The Journal of Biological Chemistry*, *282*(42), 30763–75. http://doi.org/10.1074/jbc.M704655200

Edgar, R. C. (2004). MUSCLE: multiple sequence alignment with high accuracy and high throughput. *Nucleic Acids Research*, *32*(5), 1792–7. http://doi.org/10.1093/nar/gkh340

Egerer, M., Giesemann, T., Jank, T., Satchell, K. J. F., & Aktories, K. (2007). Auto-catalytic cleavage of *Clostridium difficile* toxins A and B depends on cysteine protease activity. *The Journal of Biological Chemistry*, *282*(35), 25314–21. http://doi.org/10.1074/jbc.M703062200

Fridy, P. C., Otto, J. C., Dollins, D. E., & York, J. D. (2007). Cloning and characterization of two human VIP1-like inositol hexakisphosphate and diphosphoinositol pentakisphosphate kinases. *The Journal of Biological Chemistry*, *282*(42), 30754–62. http://doi.org/10.1074/jbc.M704656200

Fukazawa, A., Alonso, C., Kurachi, K., Gupta, S., Lesser, C. F., McCormick, B. A., & Reinecker, H.-C. (2008). GEF-H1 mediated control of NOD1 dependent NF-κB activation by *Shigella* effectors. *PLoS Pathogens*, *4*(11), e1000228. http://doi.org/10.1371/journal.ppat.1000228

Fullner, K. J., & Mekalanos, J. J. (2000). *In vivo* covalent cross-linking of cellular actin by the *Vibrio cholerae* RTX toxin. *The EMBO Journal*, *19*(20), 5315–23. http://doi.org/10.1093/emboj/19.20.5315

Grant, S. G. N., Jessee, J., Bloom, F. R., & Hanahan, D. (1990). Differential plasmid rescue from

351 transgenic mouse DNAs into *Escherichia coli* methylation-restriction mutants. *Proceedings of*
352 *the National Academy of Sciences of the United States of America*, *87*(12), 4645–9. Retrieved
353 from http://www.ncbi.nlm.nih.gov/pubmed/2162051

354 Gu, C., Wilson, M. S. C., Jessen, H. J., Saiardi, A., & Shears, S. B. (2016). Inositol Pyrophosphate
355 Profiling of Two HCT116 Cell Lines Uncovers Variation in $InsP_8$ Levels. *PloS ONE*, *11*(10),
356 e0165286. http://doi.org/10.1371/journal.pone.0165286

357 Just, I., Selzer, J., Wilm, M., von Eichel-Streiber, C., Mann, M., & Aktories, K. (1995). Glucosylation
358 of Rho proteins by *Clostridium difficile* toxin B. *Nature*, *375*(6531), 500–3.
359 http://doi.org/10.1038/375500a0

360 Kelley, L. A., Mezulis, S., Yates, C. M., Wass, M. N., & Sternberg, M. J. E. (2015). The Phyre2 web
361 portal for protein modeling, prediction and analysis. *Nature Protocols*, *10*(6), 845–858.
362 http://doi.org/10.1038/nprot.2015-053

363 Khalil, I. A., Troeger, C., Blacker, B. F., Rao, P. C., Brown, A., Atherly, D. E., … Reiner, R. C.
364 (2018). Morbidity and mortality due to *Shigella* and enterotoxigenic *Escherichia coli* diarrhoea:
365 the Global Burden of Disease Study 1990-2016. *The Lancet Infectious Diseases*, *18*(11), 1229–
366 1240. http://doi.org/10.1016/S1473-3099(18)30475-4

367 Kilari, R. S., Weaver, J. D., Shears, S. B., & Safrany, S. T. (2013). Understanding inositol
368 pyrophosphate metabolism and function: kinetic characterization of the DIPPs. *FEBS Letters*,
369 *587*(21), 3464–70. http://doi.org/10.1016/j.febslet.2013.08.035

370 Labrec, E. H., Schneider, H., Magnani, T. J., & Formal, S. B. (1964). Epithlelial cell penetration as an
371 essential step in the pathogenesis of bacillary dysentery. *Journal of Bacteriology*, *88*(5), 1503–
372 18. Retrieved from http://www.ncbi.nlm.nih.gov/pubmed/16562000

373 Lee, Y.-S., Mulugu, S., York, J. D., & O'Shea, E. K. (2007). Regulation of a cyclin-CDK-CDK
374 inhibitor complex by inositol pyrophosphates. *Science*, *316*(5821), 109–12.
375 http://doi.org/10.1126/science.1139080

376 Liu, W., Zhou, Y., Peng, T., Zhou, P., Ding, X., Li, Z., … Shao, F. (2018). *N*$^{\varepsilon}$-fatty acylation of
377 multiple membrane-associated proteins by *Shigella* IcsB effector to modulate host function.
378 *Nature Microbiology*, *3*(9), 996–1009. http://doi.org/10.1038/s41564-018-0215-6

379 Lu, R., Herrera, B. B., Eshleman, H. D., Fu, Y., Bloom, A., Li, Z., … Goldberg, M. B. (2015).
380 *Shigella* Effector OspB Activates mTORC1 in a Manner That Depends on IQGAP1 and
381 Promotes Cell Proliferation. *PLoS Pathogens*, *11*(10), e1005200.
382 http://doi.org/10.1371/journal.ppat.1005200

383 Lupardus, P. J., Shen, A., Bogyo, M., & Garcia, K. C. (2008). Small molecule-induced allosteric
384 activation of the *Vibrio cholerae* RTX cysteine protease domain. *Science*, *322*(5899), 265–8.
385 http://doi.org/10.1126/science.1162403

386 Mittal, R., Peak-Chew, S. Y., Sade, R. S., Vallis, Y., & McMahon, H. T. (2010). The acetyltransferase
387 activity of the bacterial toxin YopJ of *Yersinia* is activated by eukaryotic host cell inositol
388 hexakisphosphate. *The Journal of Biological Chemistry*, *285*(26), 19927–34.
389 http://doi.org/10.1074/jbc.M110.126581

390 Mulugu, S., Bai, W., Fridy, P. C., Bastidas, R. J., Otto, J. C., Dollins, D. E., … York, J. D. (2007). A
391 conserved family of enzymes that phosphorylate inositol hexakisphosphate. *Science*, *316*(5821),
392 106–9. http://doi.org/10.1126/science.1139099

393 Prochazkova, K., & Satchell, K. J. F. (2008). Structure-function analysis of inositol
394 hexakisphosphate-induced autoprocessing of the *Vibrio cholerae* multifunctional autoprocessing
395 RTX toxin. *The Journal of Biological Chemistry*, *283*(35), 23656–64.
396 http://doi.org/10.1074/jbc.M803334200

397 Prochazkova, K., Shuvalova, L. A., Minasov, G., Voburka, Z., Anderson, W. F., & Satchell, K. J. F.
398 (2009). Structural and molecular mechanism for autoprocessing of MARTX toxin of *Vibrio*
399 *cholerae* at multiple sites. *The Journal of Biological Chemistry*, *284*(39), 26557–68.
400 http://doi.org/10.1074/jbc.M109.025510

401 Pruitt, R. N., Chagot, B., Cover, M., Chazin, W. J., Spiller, B., & Lacy, D. B. (2009). Structure-
402 function analysis of inositol hexakisphosphate-induced autoprocessing in *Clostridium difficile*
403 toxin A. *The Journal of Biological Chemistry*, *284*(33), 21934–40.
404 http://doi.org/10.1074/jbc.M109.018929

405 Pulloor, N. K., Nair, S., McCaffrey, K., Kostic, A. D., Bist, P., Weaver, J. D., … Krishnan, M. N.
406 (2014). Human genome-wide RNAi screen identifies an essential role for inositol
407 pyrophosphates in Type-I interferon response. *PLoS Pathogens*, *10*(2), e1003981.
408 http://doi.org/10.1371/journal.ppat.1003981

409 Reineke, J., Tenzer, S., Rupnik, M., Koschinski, A., Hasselmayer, O., Schrattenholz, A., … von
410 Eichel-Streiber, C. (2007). Autocatalytic cleavage of Clostridium difficile toxin B. *Nature*,
411 *446*(7134), 415–9. http://doi.org/10.1038/nature05622

412 Reinke, A., Chen, J. C.-Y., Aronova, S., & Powers, T. (2006). Caffeine targets TOR complex I and
413 provides evidence for a regulatory link between the FRB and kinase domains of Tor1p. *The*
414 *Journal of Biological Chemistry*, *281*(42), 31616–26. http://doi.org/10.1074/jbc.M603107200

415 Safrany, S. T., Ingram, S. W., Cartwright, J. L., Falck, J. R., McLennan, A. G., Barnes, L. D., &
416 Shears, S. B. (1999). The diadenosine hexaphosphate hydrolases from *Schizosaccharomyces*
417 *pombe* and *Saccharomyces cerevisiae* are homologues of the human diphosphoinositol
418 polyphosphate phosphohydrolase. *The Journal of Biological Chemistry*, *274*(31), 21735–40.
419 http://doi.org/10.1074/jbc.274.31.21735

420 Saiardi, A., Caffrey, J. J., Snyder, S. H., & Shears, S. B. (2000). The inositol hexakisphosphate kinase
421 family. Catalytic flexibility and function in yeast vacuole biogenesis. *The Journal of Biological*
422 *Chemistry*, *275*(32), 24686–92. http://doi.org/10.1074/jbc.M002750200

423 Saiardi, A., Erdjument-Bromage, H., Snowman, A. M., Tempst, P., & Snyder, S. H. (1999). Synthesis
424 of diphosphoinositol pentakisphosphate by a newly identified family of higher inositol
425 polyphosphate kinases. *Current Biology*, *9*(22), 1323–6. http://doi.org/10.1016/s0960-
426 9822(00)80055-x

427 Savidge, T. C., Urvil, P., Oezguen, N., Ali, K., Choudhury, A., Acharya, V., … Pothoulakis, C.
428 (2011). Host *S*-nitrosylation inhibits clostridial small molecule-activated glucosylating toxins.
429 *Nature Medicine*, *17*(9), 1136–41. http://doi.org/10.1038/nm.2405

430 Schindelin, J., Arganda-Carreras, I., Frise, E., Kaynig, V., Longair, M., Pietzsch, T., … Cardona, A.
431 (2012). Fiji: an open-source platform for biological-image analysis. *Nature Methods*, *9*(7), 676–
432 82. http://doi.org/10.1038/nmeth.2019

433 Sheahan, K., Cordero, C. L., & Satchell, K. J. F. (2007). Autoprocessing of the *Vibrio cholerae* RTX
434 toxin by the cysteine protease domain. *The EMBO Journal*, *26*(10), 2552–61.
435 http://doi.org/10.1038/sj.emboj.7601700

436 Shears, S. B. (2018). Intimate connections: Inositol pyrophosphates at the interface of metabolic
437 regulation and cell signaling. *Journal of Cellular Physiology*, *233*(3), 1897–1912.
438 http://doi.org/10.1002/jcp.26017

439 Shen, A., Lupardus, P. J., Gersch, M. M., Puri, A. W., Albrow, V. E., Garcia, K. C., & Bogyo, M.
440 (2011). Defining an allosteric circuit in the cysteine protease domain of *Clostridium difficile*
441 toxins. *Nature Structural & Molecular Biology*, *18*(3), 364–71.
442 http://doi.org/10.1038/nsmb.1990

443 Slagowski, N. L., Kramer, R. W., Morrison, M. F., LaBaer, J., & Lesser, C. F. (2008). A functional
444 genomic yeast screen to identify pathogenic bacterial proteins. *PLoS Pathogens*, *4*(1), e9.
445 http://doi.org/10.1371/journal.ppat.0040009

446 Sopko, R., Huang, D., Preston, N., Chua, G., Papp, B., Kafadar, K., … Andrews, B. (2006). Mapping
447 pathways and phenotypes by systematic gene overexpression. *Molecular Cell*, *21*(3), 319–30.
448 http://doi.org/10.1016/j.molcel.2005.12.011

449 Steidle, E. A., Chong, L. S., Wu, M., Crooke, E., Fiedler, D., Resnick, A. C., & Rolfes, R. J. (2016).
450 A novel inositol pyrophosphate phosphatase in *Saccharomyces cerevisiae*: Siw14 protein
451 selectively cleaves the β-phosphate from 5-diphosphoinositol pentakisphosphate (5PP-IP_5). *The*

452 *Journal of Biological Chemistry*, *291*(13), 6772–83. http://doi.org/10.1074/jbc.M116.714907

453 Szijgyarto, Z., Garedew, A., Azevedo, C., & Saiardi, A. (2011). Influence of inositol pyrophosphates
454 on cellular energy dynamics. *Science*, *334*(6057), 802–5. http://doi.org/10.1126/science.1211908

455 Wang, H., Gu, C., Rolfes, R. J., Jessen, H. J., & Shears, S. B. (2018). Structural and biochemical
456 characterization of Siw14: A protein-tyrosine phosphatase fold that metabolizes inositol
457 pyrophosphates. *The Journal of Biological Chemistry*, *293*(18), 6905–6914.
458 http://doi.org/10.1074/jbc.RA117.001670

459 York, J. D., Odom, A. R., Murphy, R., Ives, E. B., & Wente, S. R. (1999). A phospholipase C-
460 dependent inositol polyphosphate kinase pathway required for efficient messenger RNA export.
461 *Science*, *285*(5424), 96–100. Retrieved from http://www.ncbi.nlm.nih.gov/pubmed/10390371

462 Zurawski, D. V., Mumy, K. L., Faherty, C. S., McCormick, B. A., & Maurelli, A. T. (2009). *Shigella*
463 *flexneri* type III secretion system effectors OspB and OspF target the nucleus to downregulate
464 the host inflammatory response *via* interactions with retinoblastoma protein. *Molecular*
465 *Microbiology*, *71*(2), 350–68. http://doi.org/10.1111/j.1365-2958.2008.06524.x

466

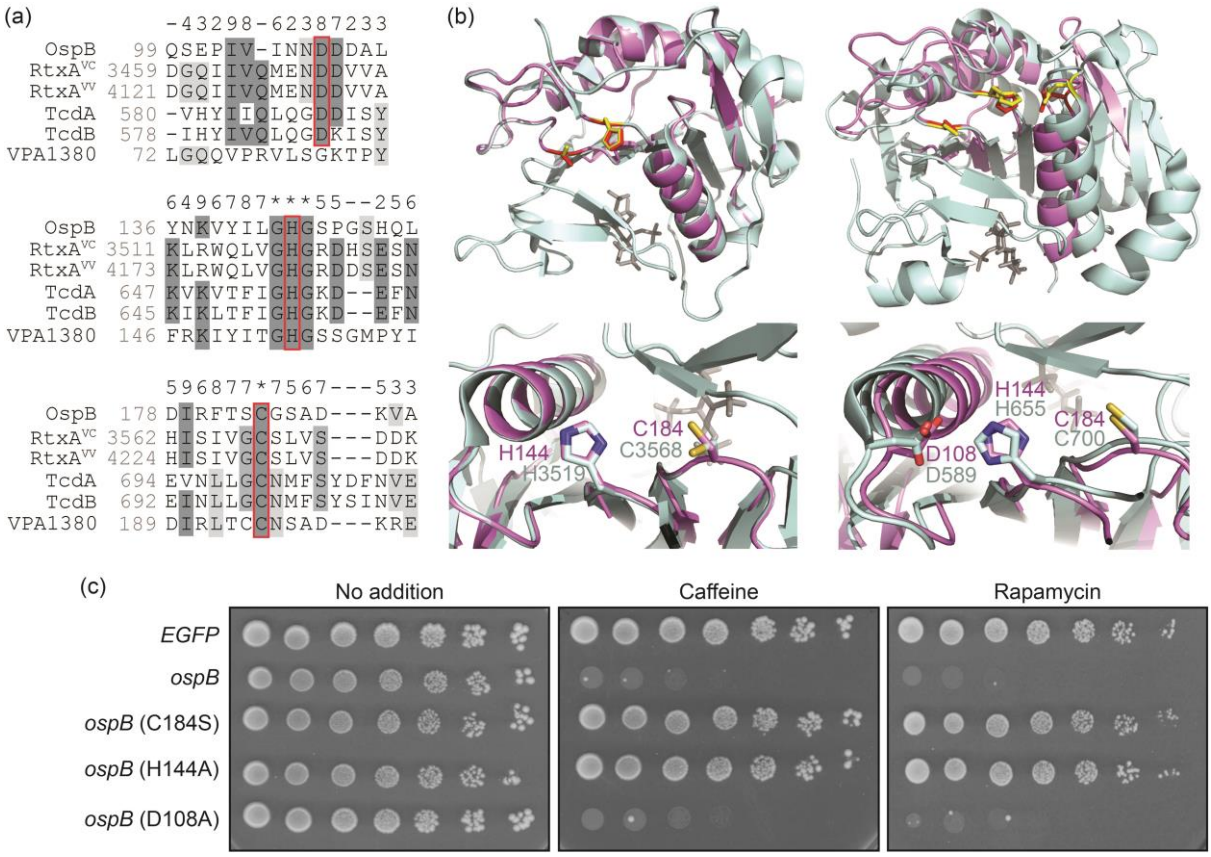

Figure 1: Prediction of catalytic residues of OspB. (a) Multiple sequence alignment of OspB with the catalytic residues of the cysteine protease domains of RtxA from *V. cholerae* ($RtxA^{VC}$) and *V. vulnificus* ($RtxA^{VV}$), *C. difficile* TcdA and TcdB, and the OspB ortholog VPA1380 from *V. parahaemolyticus*. Red boxes indicate catalytic residues of the cysteine protease domains and the aligned putative catalytic residues of OspB. Darkness of gray shading reflects the conservation of individual residues, and the numbers above the alignment score the conservation at each position. Asterisks denote full conservation among the aligned sequences. (b) Cartoon depictions of a tertiary structure model of OspB (violet) on the CPDs of $RtxA^{VC}$ (*left panels*; PDB: 3EEB) and TcdA (*right panels*; PDB: 3HO6) (pale cyan). In the top panels, the catalytic residues of the cysteine protease domains are denoted by yellow sticks, with the putative catalytic residues of OspB shown as red sticks. IP_6 in the $RtxA^{VC}$ and TcdB cysteine protease domain structures is shown in dark gray. Enlarged and rotated views show the active sites (*bottom panels*), highlighting the superposition of the putative OspB catalytic residues with those of the cysteine protease domains, labelled according to the color of the cartoon. (c) Growth of yeast strains expressing *ospB* constructs or an *EGFP* control. Serial dilutions

482 were spotted on media either without additives or supplemented with the TOR inhibitors caffeine
483 (6 mM) or rapamycin (5 nM). Images are representative of three independent replicates.

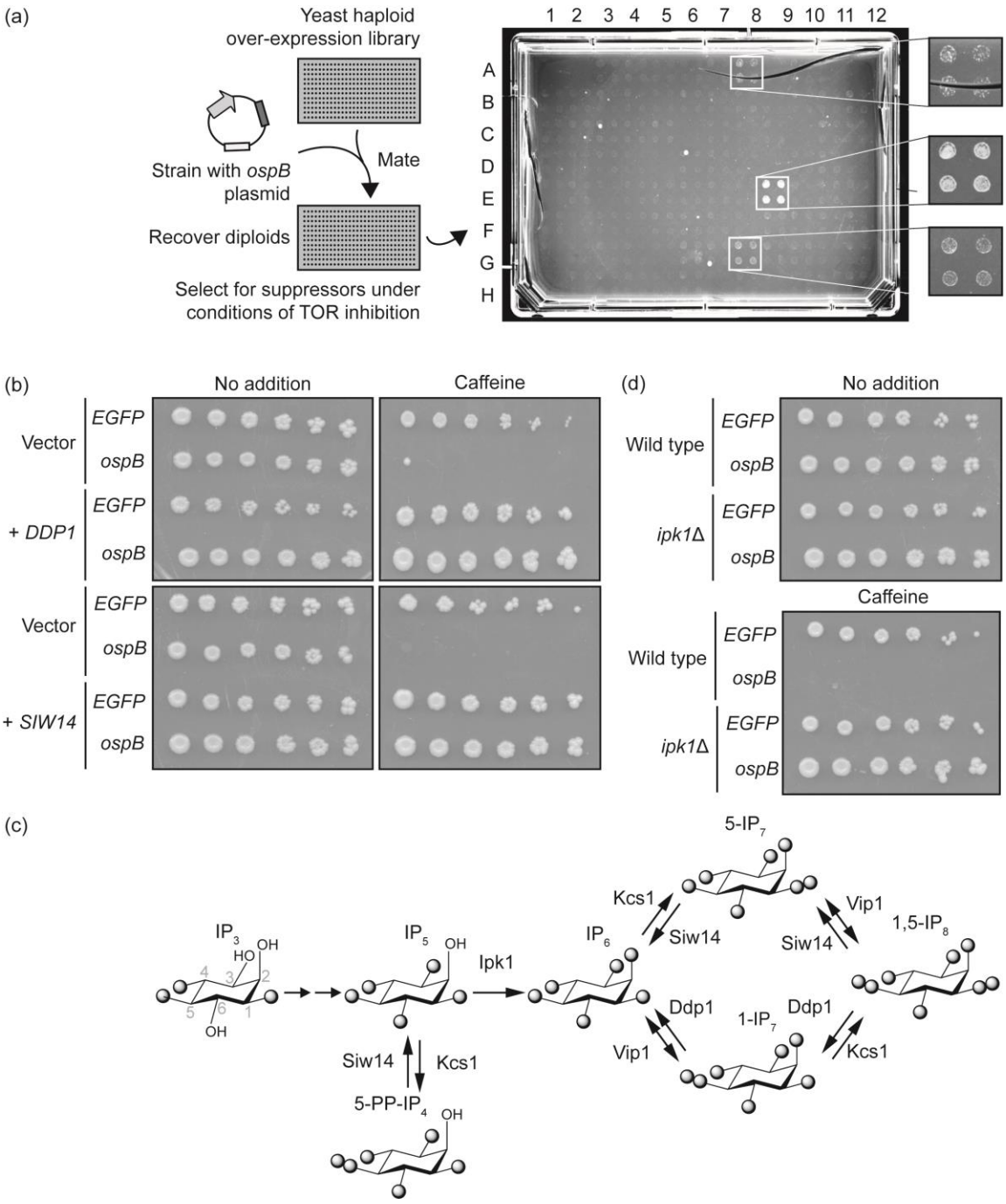

Figure 2: A yeast suppressor screen reveals a role of inositol pyrophosphates in OspB activity. (a) Schematic of the over-expression library screen designed to identify suppressors of OspB-mediated growth inhibition in the presence of caffeine (See Experimental Procedures for details). An example of a quad-spotted output plate is shown, with three hits magnified. (b) Impact of multi-copy over-expression of *DDP1* or *SIW14* on growth of yeast strains that express *ospB* or an *EGFP* control. Serial dilutions were spotted in the presence or absence of the TOR inhibitor caffeine. Images are

491 representative of four independent replicates. (c) Schematic of the yeast soluble inositol phosphate
492 biosynthetic pathway, with the kinase and phosphatase that catalyze each step indicated (dark gray
493 lettering). The species names are shown in bold lettering. (d) Impact of deletion of *ipk1* on growth of
494 yeast strains that express *ospB* or an *EGFP* control. Serial dilutions were spotted on media with or
495 without caffeine. Images are representative of four independent replicates.

496

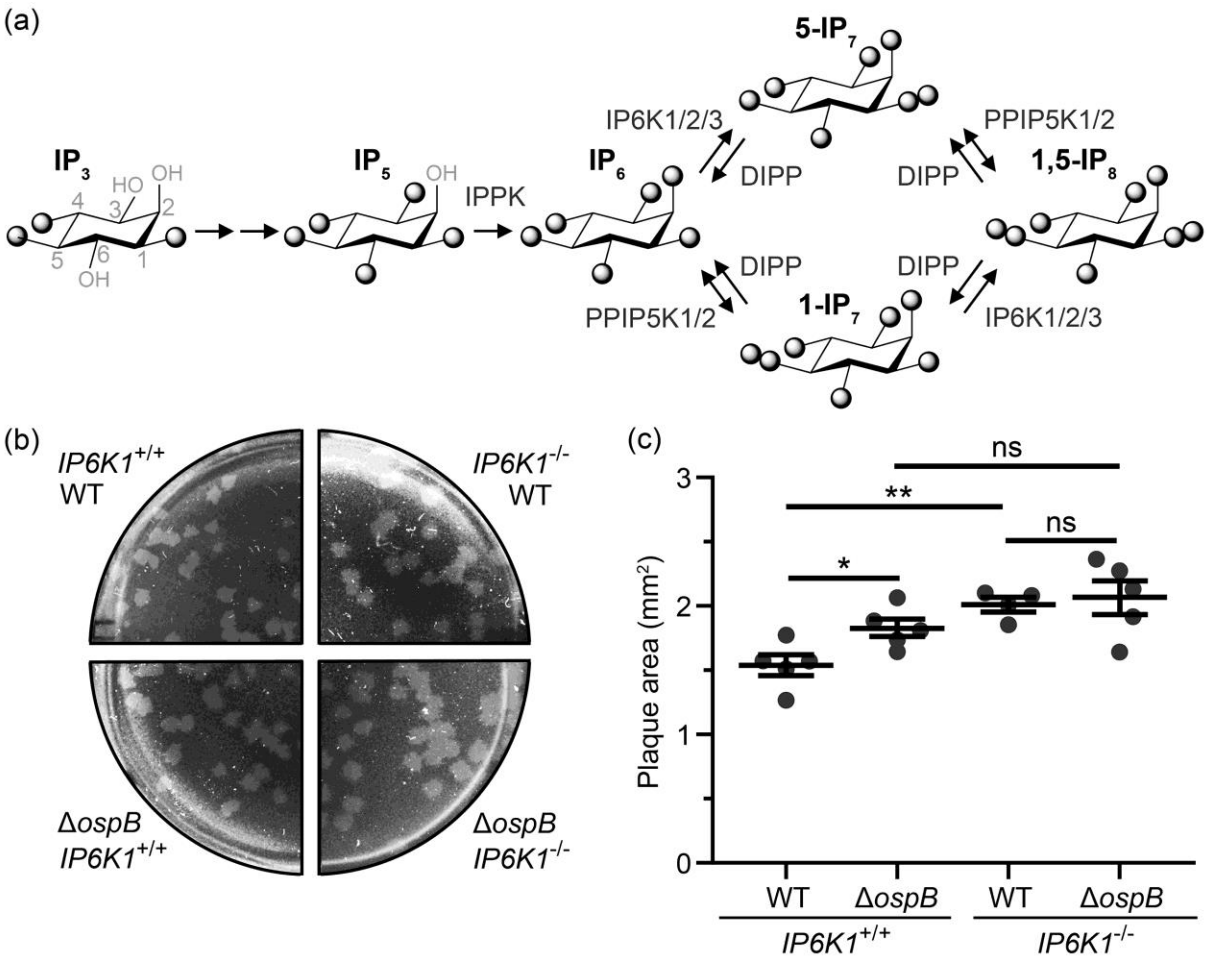

Figure 3: Inositol pyrophosphate synthesis in mammalian cells alters activity of OspB during *S. flexneri* infection. (a) Schematic of the mammalian inositol phosphate biosynthetic pathway. Several isoforms of enzymes are present at many positions in the pathway (dark gray lettering). Of note, it is thought that the generation of 1,5-IP_8 from IP_6 primarily proceeds *via* 5-IP_7, whereas most 1-IP_7 is thought to be synthesized from 1,5-IP_8 (Gu et al., 2016). The species names are shown in bold lettering. (b-c) Impact of deletion of *IP6K1* on *S. flexneri* spread through cell monolayers. Infection of *IP6K1*-deficient mouse embryonic fibroblasts and littermate-derived wild type control cells with wild type *S. flexneri* or an isogenic Δ*ospB* mutant. Representative images of plaques (b) and quantification of plaque area (c). Data are from at least 4 independent experiments. Two-tailed Student's *t*-test: * $p < 0.05$; ** $p < 0.01$; ns, not significant).

Supporting Information

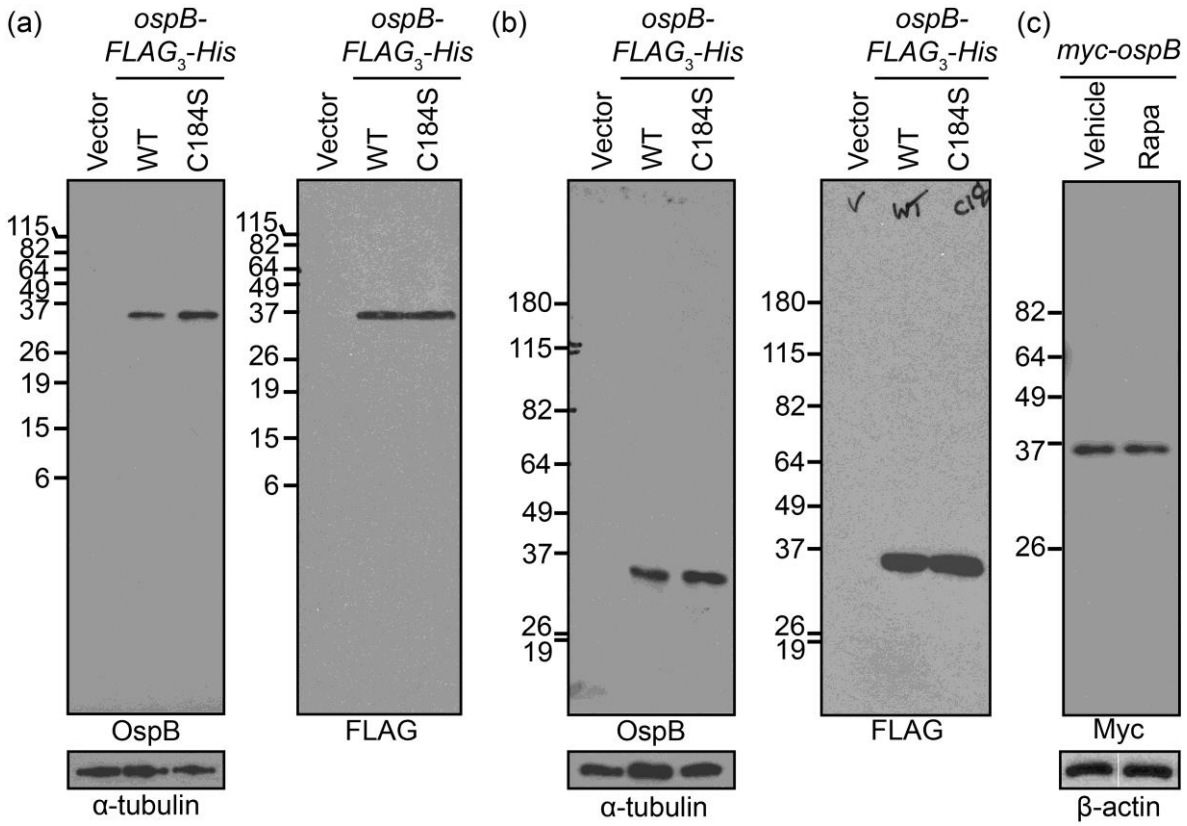

Figure S1. Absence of evidence of processing of OspB in cell lysates. (a) Wild type OspB and OspB (C184S) expressed in yeast, detected by immunoblotting with anti-OspB and anti-FLAG antibodies after separation on a 15% SDS-PAGE gel. α-tubulin serves as a loading control. (b) Samples from panel (a) separated on a 7.5% SDS-PAGE gel and probed as in panel (a). (c) Transfection of mouse embryonic fibroblasts with pCMV-*myc-ospB*. Cells were treated with rapamycin (10 nM) (+) or a DMSO vehicle control. Myc-OspB detected by immunoblotting with an anti-myc antibody after separation on a 10% SDS-PAGE gel. β-actin serves as the loading control; bands from a single blot.

519 **Table S1: Yeast genes whose over-expression suppresses OspB-mediated growth inhibition of *S.***

520 ***cerevisiae* in the presence of caffeine.**

521 The functions of the gene products are from the *Saccharomyces* genome database (Cherry et al., 2012).

522 Genes are listed alphabetically by name.

Name	Gene	Function of gene product
BRE1	*YDL074C*	E3 ubiquitin ligase
CLN3	*YAL040C*	Regulatory subunit of cyclin-dependent protein kinase
COS3	*YML132W*	Membrane protein turnover
CSM1	*YCR086W*	Nucleolar protein involved in meiosis
CYC3	*YAL039C*	Holocytochrome *c* synthase
DDI1	*YER143W*	SNARE-binding protein
DDP1	*YOR163W*	Inositol pyrophosphate pathway phosphatase
EMA17	*YIL029C*	Putative protein of unknown function
FMT1	*YBL013W*	Methionyl-tRNA formyltransferase
GAL11	*YOL051W*	Subunit of RNA polymerase II mediator complex
HIS3	*YOR202W*	Histidine biosynthesis
HSP60	*YLR259C*	Mitochondrial chaperonin
JJJ3	*YJR097W*	Putative protein of unknown function
LAT1	*YNL071W*	Subunit of pyruvate dehydrogenase complex
LSB1	*YGR136W*	Negative regulator of actin nucleation
MTC6	*YHR151C*	Putative protein of unknown function
PBY1	*YBR094W*	Putative tubulin tyrosine ligase
PPE1	*YHR075C*	Carboxyl methyl esterase
PRX1	*YBL064C*	Mitochondrial thioredoxin peroxidase
PTC3	*YBL056W*	Type 2C protein phosphatase (PP2C)
QCR6	*YFR033C*	Subunit of cytochrome bc_1 complex

RIM11	*YMR139W*	Protein kinase
SEC3	*YER008C*	Subunit of the exocyst complex
SIW14	*YNL032W*	Inositol pyrophosphate pathway phosphatase
SLX8	*YER116C*	Subunit of SUMO-targeted ubiquitin ligase complex
TCB1	*YOR086C*	Endoplasmic reticulum-plasma membrane tethering
TKL2	*YBR117C*	Transketolase in the pentose phosphate pathway
UBC1	*YDR177W*	Ubiquitin conjugating enzyme
UMP1	*YBR173C*	Chaperone
YUH1	*YJR099W*	Thiol-dependent ubiquitin-specific protease
-	*YAR023C*	Putative protein of unknown function
-	*YBL100C*	Putative protein of unknown function
-	*YBR116C*	Putative protein of unknown function
-	*YBR284W*	Putative metal-dependent hydrolase

523

524